iLeg—A Lower Limb Rehabilitation Robot: A Proof of Concept

Feng Zhang, Zeng-Guang Hou, Long Cheng, Weiqun Wang, Yixiong Chen, Jin Hu, Liang Peng, and Hongbo Wang

***Abstract*—In this paper, a robot, namely *iLeg*, is designed for the purpose of rehabilitation of patients with hemiplegia or paraplegia. The *iLeg* is composed of one reclining seat and two leg orthoses, and each leg orthosis has three degrees of freedom, which correspond to the hip, knee, and ankle. Based on this robotic system, two controllers, i.e., passive training controller and active training controller, are proposed. The former takes advantage of the proportional-integral control method to solve the trajectory tracking problem, and the latter employs the surface electromyography signals to achieve active training. Two simplified impedance controllers, i.e., damping-type velocity controller and spring-type position controller, are designed for active training. A perceptron neural network detects movement intentions. The performance of the controllers was investigated with one able-bodied male. The results showed that the leg orthosis tracked the predefined trajectory based on the passive training controller, with the error rates of 0.45%, 0.44%, and 0.27%, respectively, for the hip, knee, and ankle. The active training controller whose loop rate is 6.67 Hz can move the leg orthosis smoothly, and the average recognition error of the perceptron neural network is less than 5%.**

***Index Terms*—Active training, electromyography (EMG), rehabilitation robot, spinal cord injury (SCI).**

I. Introduction

STROKE and spinal cord injury (SCI) often lead to long-term limb dysfunctions, especially hemiplegia and paraplegia. To improve neurorehabilitation and motor recovery, and to avoid disuse atrophy of the lower limbs, repetitive and intensive rehabilitation exercises with the disabled limbs are indispensable. Traditional rehabilitation exercises that are conducted manually with the help of therapists are not only labor intensive, but also very costly. Rehabilitation bikes are often used in China to help stroke or SCI patients do treadmill training, which has a positive role on activities of daily living in convalescent stroke patients [1]. The lower limb rehabilitation robot (LLRR) could provide a more flexible alternative to rehabilitation bikes.

Manuscript received December 17, 2014; revised April 25, 2015, October 21, 2015, and January 10, 2016; accepted April 8, 2016. Date of publication July 7, 2016; date of current version September 14, 2016. This work was supported in part by the National Natural Science Foundation of China under Grant 61225017, Grant 61403378, Grant 61422310, Grant 61421004, and Grant 61533016, and by the Strategic Priority Research Program of the Chinese Academy of Sciences under Grant XDB02080000. This paper was recommended by Associate Editor J. L. Contreras-Vidal. *(Corresponding author: Zeng-Guang Hou.)*

F. Zhang, Z.-G. Hou, L. Cheng, W. Wang, Y. Chen, J. Hu, and L. Peng are with the State Key Laboratory of Management and Control for Complex Systems, Institute of Automation, Chinese Academy of Sciences, Beijing 100190, China (e-mail: feng.zhang@ia.ac.cn; zengguang.hou@ia.ac.cn; long.cheng@ia.ac.cn; weiqun.wang@ia.ac.cn; yixiong.chen@ia.ac.cn; jin.hu@ia.ac.cn; liang.peng@ia.ac.cn).

H. Wang is with the School of Mechanical Engineering, Yanshan University, Qinhuangdao 066004, China (e-mail: hongbo_w@ysu.edu.cn).

Color versions of one or more of the figures in this paper are available online at http://ieeexplore.ieee.org.

Digital Object Identifier 10.1109/THMS.2016.2562510

The LLRRs can be categorized into three types according to their driving mechanisms and locomotor training styles. The first one is the sitting/lying type that features a reclining seat and two leg orthoses, e.g., MotionMaker [2]. It can be used for single- and multiple-joint rehabilitation. The second one is the standing/walking type that usually comprises a step-posture control system and a body weight support system, e.g., Lokomat [3], LOPES [4], LokoHelp [5], ReoAmbulator [6], Gait Trainer [7], HapticWalker [8], and WalkTrainer [9]. This type of LLRR assists walking movements of gait-impaired patients and combines intensive functional locomotion therapy with patient assessment and feedback tools. The third one is the wearable exoskeleton type that can be worn by the patient and assists him/her to stand or walk, e.g., Ekso [10], Rex [11], Robot Suit HAL [12], and ReWalk [13]. The effectiveness of LLRR is still an open topic in the current literature. While some studies show their effectiveness [3], [15], [16], other studies suggest that robotics are not superior to traditional physical therapy [14].

The sitting/lying-type LLRR could provide a useful alternative to rehabilitation bikes, as it can help patients do not only passive treadmill training, but also other types of training, such as active training or functional electrical stimulation (FES). For example, the MotionMaker™ takes advantage of FES to mimic natural exercise during the rehabilitation [16].

Voluntary or active motor training has been proven more beneficial than passive motor training in eliciting performance improvements and cortical reorganization [17]; thus, an LLRR that can help patients accomplish not only passive training, but also active training would be more helpful. Electromyography (EMG) that contains rich information of muscle activity and voluntary intention can be used for this purpose. For example, Leonard *et al.* developed a novel EMG-driven hand exoskeleton for bilateral rehabilitation of grasping in stroke, and the EMG signals from the nonparetic hand were used to estimate the grasping force and then replicated as robotic assistance for the paretic hand by means of the hand-exoskeleton [18]. Studies also suggest that substantial motor control information can be extracted from paretic muscles of stroke survivors by EMG signals [19].

In this study, we introduce a novel sitting/lying-type LLRR, namely *iLeg*. *iLeg* is intended for handicapped and hemiplegic patients, and its main functions are training and rehabilitation of articular mobility and movement coordination, as well as muscular strength. The purpose of developing *iLeg* is to replace rehabilitation bikes and provide more rehabilitation training methods. Two rehabilitation training control methods, i.e., passive training and active training, are proposed. Two simplified impedance control methods, i.e., spring-type position control and damping-type velocity control based on EMG signals, are implemented to control the robot's motion. Finally,

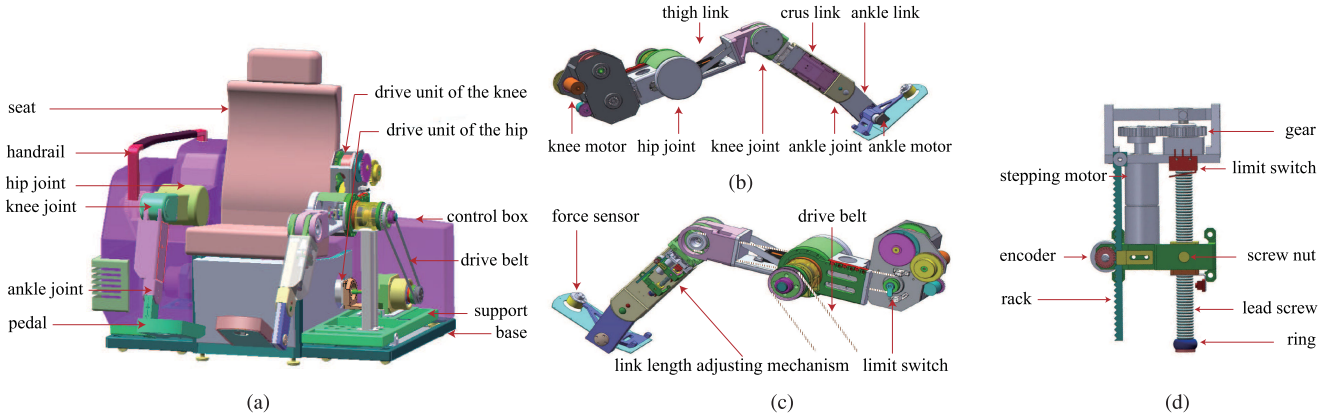

Fig. 1. Mechanism of *iLeg*. (a) Virtual prototype of *iLeg*. (b) Interior view of left leg orthosis mechanism. (c) Exterior view of left leg orthosis mechanism. (d) Crus length adjusting mechanism.

TABLE I
ADJUSTMENT RANGES OF *iLeg*

Item	Width	Thigh link	Crus link	Ankle link
Minimum (mm)	400	315	325	90
Maximum (mm)	540	395	420	90

TABLE II
JOINT ANGLE RANGES AND SPECIFICATIONS OF THE MOTORS OF *iLeg*

Item	Minimal (°)	Maximal (°)	Torque (N·m)	Speed (r/min)	Power (W)	Reduction
Hip	0	80	1.333	3200	447	120
Knee	−120	0	0.55	4860	280	180
Ankle	−15	35	0.09	8600	79.4	190

the system performance is investigated in a proof-of-concept evaluation.

II. SYSTEM DESIGN

A. Mechanical System Design

The virtual prototype of *iLeg*, which consists of one reclining seat, two leg orthoses, two support mechanisms, one control box, and a base, is shown in Fig. 1(a). The modular-design supports assembling, debugging, and maintenance of *iLeg*. The seat back can be adjusted to an optional angle between 90° and 160°; thus, the patient can sit or recline in the seat. Each leg orthosis is mounted on an associated support mechanism, which can move bidirectionally on the base; thus, the distance between two leg orthoses can be adjusted. The distance is defined as the width of *iLeg* (see Table I). It is adjusted to be consistent with the hip width of the patient during training. The maximum adjustment facilitates getting ON and OFF.

B. Leg Orthosis

The two leg orthoses' mechanical structures are symmetrical. The virtual prototype of the left leg orthosis is shown in Fig. 1(b) and (c). Each leg orthosis has three degrees of freedom, which correspond to the hip, knee, and ankle. The leg orthosis can simulate leg movements such as hip flexion/extension, knee flexion/extension, ankle flexion/extension, and the coordinated movements of the three joints. By considering the physiological movement range of each joint of human leg [20], the movement ranges of *iLeg* are given in Table II.

Each joint of the orthosis is driven by a DC servo motor, and drive belts are used for energy transmission. By using the drive belt, the motors can be located far away from the associated joints; thus, the mechanical structures of the thigh and crus links can be smaller. Mechanical interference between the drive units and robot links is eliminated. The ankle motor (32SYK60 of Saegmotory Co., Ltd., Shanghai, China) is located in the pedal, and its output power is delivered to the ankle through a driving belt which is hidden in the ankle link [see Fig. 1(b)]. This addresses the limited space in the ankle. The hip and knee joints are also driven this way. The drive unit of the knee is located behind the hip joint. This novel design not only reduces the size and complexity of the joint, but also offsets some weight of the leg orthosis. The knee motor (48SYK91 of Saegmotory Co., Ltd., Shanghai, China) speed of the orthosis is reduced through the harmonic transmission and multistage gear mechanism, increasing output torque. The drive unit of the hip is placed on the associated support mechanism to simplify the mechanical structure of the orthosis, as shown in Fig. 1(a). The hip motor (ID33004 of MCG, Inc., MN, USA) speed is reduced through a harmonic speed reducer, and then, the power is delivered to the hip through a driving belt. The specifications of the motors of *iLeg* are given in Table II.

C. Adjusting Mechanism

The link length of the leg orthosis should be adjustable to fit patients of different height (150–190 cm). *iLeg* can adjust lengths of the thigh and crus by the associated electric length

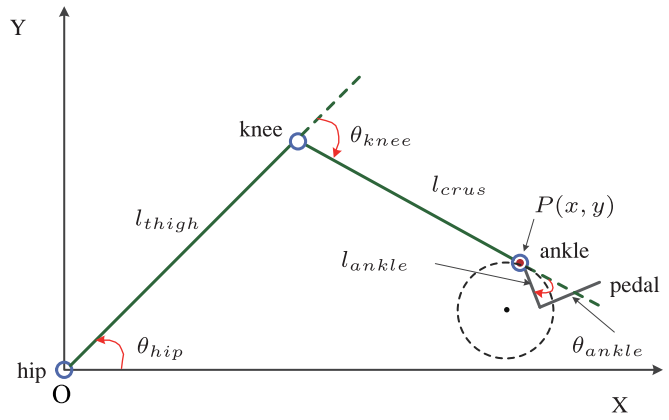

Fig. 2. Kinematic model of the leg orthosis.

adjusting mechanism; thus, the leg orthosis somewhat matches the human leg. According to the respective proportion of thigh and crus lengths to body height [21], the designed adjustment ranges of each link are given in Table I. The length adjusting mechanisms are implemented through telescopic mechanisms, and each link can be controlled in a sliding groove to change the length. The lead screw that is driven by a stepping motor and associated screw nut is used to drive the mechanisms. The prototype of the drive unit of the crus length adjusting mechanism is shown in Fig. 1(d). The encoder in Fig. 1(d) is used to measure the link length, and it moves together with the screw nut along the rack. Limit switches are used to detect the limit positions. One end of the crus length adjusting mechanism is fixed to the knee joint, and the other end is connected to the crus link through the screw nut. The thigh length adjusting mechanism uses a similar idea, although it is implemented differently. By using this driving method, the length adjusting mechanisms move stably and smoothly. The ankle link shown in Fig. 1(b) is the segment between the ankle joint and the pedal, and it corresponds to the patient's foot height. As there is no adjusting mechanism, layers on the pedal can support patients with different foot heights.

III. Control Methods

A. Kinematics

The leg orthosis has three serial links: thigh, crus, and ankle [see Fig. 1(b)]. The kinematic model of the leg orthosis is shown in Fig. 2. The hip joint angle is 0° when the thigh is parallel to the seat plane. Trajectory planning of the leg orthosis in the Cartesian plane usually refers to the trajectory of point P which is at the end of the crus link. The movement of the ankle joint is often planned according to specific applications. For example, for passive cycling training, the trajectory of point P is a circle in the Cartesian plane, while the ankle joint can keep still during the cycling movement. Thus, a simplified two-link model can be used for the kinematic analysis of the leg orthosis.

We obtain the forward kinematics of leg orthosis as

$$\begin{aligned} x &= l_{\text{thigh}}\cos(\theta_{\text{hip}}) + l_{\text{crus}}\cos(\theta_{\text{hip}}+\theta_{\text{knee}}) \\ y &= l_{\text{thigh}}\sin(\theta_{\text{hip}}) + l_{\text{crus}}\sin(\theta_{\text{hip}}+\theta_{\text{knee}}) \end{aligned} \tag{1}$$

where x and y denote the coordinates of point P, l_{thigh} and l_{crus} are the lengths of thigh and crus links, and θ_{hip} and θ_{knee} are the joint angles of hip and knee, respectively. According to (1), we obtain the inverse kinematics of leg orthosis as

$$\begin{aligned} \theta_{\text{hip}} &= \arctan\frac{y}{x} + \arccos\frac{l_{\text{thigh}}^2 - l_{\text{crus}}^2 + x^2 + y^2}{2l_{\text{thigh}}\sqrt{x^2+y^2}} \\ \theta_{\text{knee}} &= -\arccos\frac{x^2+y^2-l_{\text{thigh}}^2-l_{\text{crus}}^2}{2l_{\text{thigh}}l_{\text{crus}}}. \end{aligned} \tag{2}$$

By (2), we can obtain the joint trajectories once the trajectory of point P is known.

B. Passive Training Controller

The passive training controller solves the trajectory tracking problem of the leg orthosis. A proportional-integral (PI) controller is designed in the motor driver layer for this purpose. The PI controller is composed of the current loop, velocity loop, and position loop (see Fig. 3).

The position loop is in the outer layer; it receives position command θ_d from the trajectory generator, and calculates the instantaneous profile velocity $\dot{\theta}_d$ and acceleration $\ddot{\theta}_d$. These signals along with the actual position feedback θ are processed by the position loop to generate a velocity command v_c. From Fig. 3, we obtain the velocity command v_c as

$$v_c = P_p(\theta_d - \theta) + V_f\dot{\theta}_d + A_f\ddot{\theta}_d \tag{3}$$

where P_p, V_f, and A_f are the proportional gain, velocity feed forward gain, and acceleration feed forward gain, respectively. The primary effect of P_p is reducing the rise time, V_f is reducing tracking error during constant velocity, and A_f is reducing tracking error during acceleration and deceleration.

The velocity loop in the middle layer accepts the velocity command which is generated by the position loop, subtracts the actual velocity v and produces a velocity error signal Δv. The error signal is processed by using the integral and proportional gains to produce a current command i_c:

$$i_c = V_p(v_c - v) + V_i\int_0^t (v_c - v)dt \tag{4}$$

where V_p and V_i are the velocity loop proportional and integral gains, respectively.

The current loop is in the inner layer, and it is similar to the velocity loop in structure. This loop tracks the current command i_c by adjusting the PWM command. The current i generated by this loop can be described by

$$i = C_p(i_c - i) + C_i\int_0^t (i_c - i)dt \tag{5}$$

where C_p and C_i are the current loop proportional and integral gains, respectively.

The parameters in the PI controller are tuned manually in a specific order: current loop, velocity loop, position loop (see Table III).

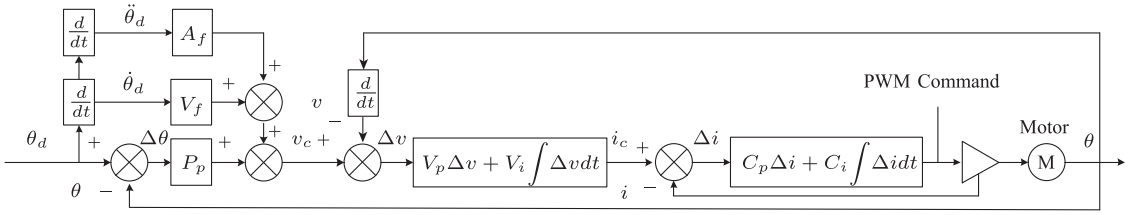

Fig. 3. Structure of the PI controller.

TABLE III
PARAMETERS OF THE PI CONTROLLER

Joint	P_P	V_f	A_f	V_p	V_i	C_p	C_i
Hip	1800	6000	16384	400	10	68	138
Knee	1500	5200	15124	500	20	100	120
Ankle	1300	4000	12571	300	15	200	158

C. Active Training Controller

1) Controller Design: For active training, the robot trajectories are controlled by the patient. The robot, *iLeg*, detects the patient's motion intention and assists him/her to achieve it. Impedance control is a popular method for active control of a manipulator's interactive behavior [22], [24]. The basic idea of impedance control is to establish a mass–damper–spring relationship between the Cartesian position Δx and the Cartesian torque/force τ as

$$\tau = M\Delta\ddot{x} + D\Delta\dot{x} + K\Delta x \tag{6}$$

with the positive-definite matrices M, D, K representing the virtual inertia, damping, and stiffness of the interactive system, respectively. These matrices can be chosen by the control system designer according to the goals to be achieved by the robot; thus, impedance control does not attempt to track motion and force trajectories but to regulate the mechanical impedance specified by a target model [24].

Force/torque signals are important but not essential for impedance control. Due to the virtuality of M, D, and K, the Cartesian torque/force τ can also be replaced with other signals. Surface electromyography (sEMG) is a physiological signal, which represents the muscle strength directly; thus, it is a suitable alternative for obtaining the Cartesian torque/force.

The human joint flexion and extension movements are controlled by two muscle groups, i.e., agonist and antagonist, whose roles are exchanged when the movement changes. Thus, sEMG signals from the two muscle groups should be acquired simultaneously, and the role of each muscle group must be recognized firstly. In this paper, the normalized amplitudes of sEMG are directly used as the Cartesian forces. Finally, we obtain the sEMG-based impedance controller for active training as

$$CA = M\Delta\ddot{\theta} + D\Delta\dot{\theta} + K\Delta\theta$$

$$C = \begin{bmatrix} c_1 & -c_2 & 0 & 0 & 0 & 0 \\ 0 & 0 & c_3 & -c_4 & 0 & 0 \\ 0 & 0 & 0 & 0 & c_5 & -c_6 \end{bmatrix}$$

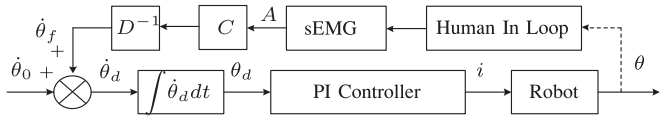

Fig. 4. Damping-type velocity controller.

$$A = \begin{bmatrix} a_1 & a_2 & a_3 & a_4 & a_5 & a_6 \end{bmatrix}^T$$
$$\theta = \begin{bmatrix} \theta_1 & \theta_2 & \theta_3 \end{bmatrix}^T \tag{7}$$

where C is a matrix classifying the agonist and antagonist of each joint; $c_i, i = 1, ..., 6$, are logical variables (0 or 1), and they correspond to the hip flexor, hip extensor, knee extensor, knee flexor, ankle flexor, and ankle extensor, respectively. If $c_i = 1$, it means that the corresponding muscle group is the agonist; otherwise, it is the antagonist. The flexor and extensor of each joint cannot be agonists at the same time. A is a vector, and $a_i, i = 1, ..., 6$, represent the normalized sEMG amplitudes of the muscles. θ is a vector, and $\theta_i, i = 1, 2, 3$, represent joint angles of the hip, knee, and ankle.

The matrices M, D, and K affect the maximum acceleration, maximum speed, and maximum position, respectively. Two simplified impedance controllers have been designed: one is the damping-type velocity controller, and the other is the spring-type position controller. The first controller is obtained by setting the matrices M and K in (7) to zero matrices, and the sEMG amplitudes are converted into joint angular velocities. Thus, the patient can drive the leg orthosis to the specific positions at different speeds by contracting the associated muscles. The control law of this method can be written as

$$CA = D(\dot{\theta}_d - \dot{\theta}_0) \tag{8}$$

where D is a positive-definite diagonal matrix, $\dot{\theta}_d$ is the desired joint angular speed, and $\dot{\theta}_0$ is the reference joint angular speed. Traditionally, $\dot{\theta}_0$ is set to a zero vector. The damping parameters in D can be adjusted to fit patients with different levels of muscle strength. When the matrix D is larger, the robot will be less sensitive to changes in sEMG. It means that more sEMG changes are necessary to achieve the same speed. The control block diagram of the damping-type velocity controller is shown in Fig. 4, from which we obtain the input of the PI controller θ_d as

$$\theta_d = \int_0^t \dot{\theta}_d dt = \int_0^t (\dot{\theta}_f + \dot{\theta}_0) dt$$
$$= \int_0^t (D^{-1}CA + \dot{\theta}_0) dt \tag{9}$$

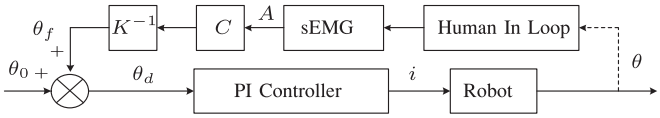

Fig. 5. Spring-type position controller.

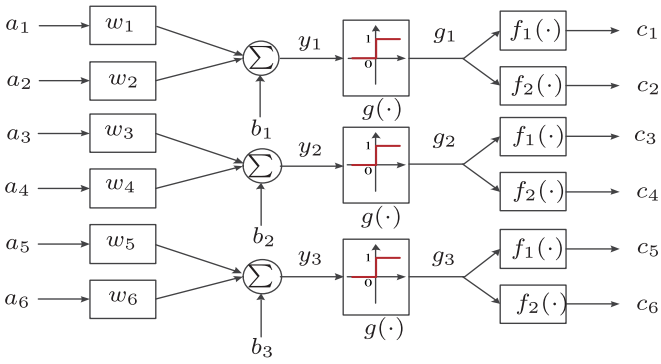

Fig. 6. Structure of the neural network.

where $\dot{\theta}_f$ is the speed command generated by the sEMG signals.

Similarly, the second controller is obtained by setting the matrices M and D in (7) to zero matrices, and the sEMG amplitudes are converted into joint angles. There is a reference angle for each joint. The orthosis deviates from the reference angle when the subject contracts the relevant muscles, and the orthosis moves back to the reference angle when the relevant muscles are relaxed. The leg orthosis works like a spring, and the control law of this method can be written as

$$CA = K(\theta_d - \theta_0) \tag{10}$$

where K is a positive-definite diagonal matrix, θ_d is the desired joint angle, and θ_0 is the reference joint angle. The stiffness parameters in K can be adjusted to fit patients with different levels of muscle strength. Similarly, when the matrix K is larger, the robot will be less sensitive to changes in sEMG. It means that more sEMG changes are necessary to achieve the same difference between θ_d and θ_0. The control block diagram of the spring-type position controller is shown in Fig. 5. According to Fig. 5 and (10), we obtain the input of the PI controller θ_d as

$$\theta_d = \theta_f + \theta_0 = K^{-1}CA + \theta_0 \tag{11}$$

where θ_f is the error between θ_d and θ_0, which is generated by the sEMG signals.

The patient is in loop of the controllers, and he/she can control the position or velocity of the leg orthosis voluntarily by contracting the agonists (see Figs. 4 and 5). Both controllers can motivate the patient to actively participate in the rehabilitation by setting appropriate training goals.

2) Agonist Recognition: Since the movements of the leg orthosis are controlled by sEMG from the agonists, the agonist recognition, namely computation of the matrix C in (7)–(11) must be completed first. Considering the independence of the joint movements, a neural network (see Fig. 6) that consists of three perceptrons with the same structure is designed for the agonist recognition.

Each perceptron has three inputs: sEMG amplitudes of the corresponding flexor and extensor, and the threshold value $b_i, i = 1, 2, 3$. The output of each perceptron can be written as

$$\begin{aligned} g_i &= g(y_i) = g\left(\sum_{j=2i-1}^{2i} w_j a_j + b_i\right) \\ &= \frac{1}{2}\left(\operatorname{sgn}\left(\sum_{j=2i-1}^{2i} w_j a_j + b_i\right) + 1\right) \\ &= \begin{cases} 1, & y_i > 0 \\ 0, & y_i \le 0, \end{cases} \quad i = 1, 2, 3. \end{aligned} \tag{12}$$

The following two linear functions $f_1(\cdot)$ and $f_2(\cdot)$ are used to obtain the outputs of the network:

$$\begin{aligned} f_1(x) &= x, \quad x = 0, 1 \\ f_2(x) &= 1 - x, \quad x = 0, 1. \end{aligned} \tag{13}$$

IV. Proof-of-Concept Prototype Evaluation

A proof-of-conceptual prototype evaluation was conducted with an able-bodied 30-year-old 175-cm-tall male. The study was approved by the Institutional Review Board of China Rehabilitation Center (Beijing, China). The experiments include passive training and active training, and all were conducted under the guidance of physician.

A. Passive Training

The purpose of passive training evaluation is to test the trajectory tracking performance of the PI controller. Because cycling training can dramatically improve aerobic capacity and functional performance of stroke patients [25], [26], the leg orthosis is controlled to follow a predefined cycling movement in this experiment.

For cycling movement, the trajectory of point $P(x, y)$, shown in Fig. 2, is a circle, which can be described as

$$\begin{aligned} x &= x_c + r\cos(\omega t) \\ y &= y_c + r\sin(\omega t) \end{aligned} \tag{14}$$

with (x_c, y_c) the center's coordinates, r the radius, and ω the angular velocity. There is a phase difference of 180° between two leg orthoses.

By substituting (14) into (2), we can obtain trajectories of the hip and knee joints. The trajectory of ankle joint is planned as that of the hip, except that the amplitude is reduced by half. Such planning can result in the ankle flexion when the ankle approaches the hip, and ankle extension when the ankle leaves the hip.

The thigh and crus links lengths were adjusted to the subject's height, in this case, $l_{\text{thigh}} = 48$ cm, $l_{\text{crus}} = 42$ cm. In this experiment, $(x_c, y_c) = (65, 0)$ cm, $r = 15$ cm, and $\omega = -0.5\,\pi/\text{s}$. Trajectory tracking performance is summarized in Fig. 7. The predefined and actual trajectories of each joint are shown in Fig. 7(a); each joint moves smoothly and follows the predefined

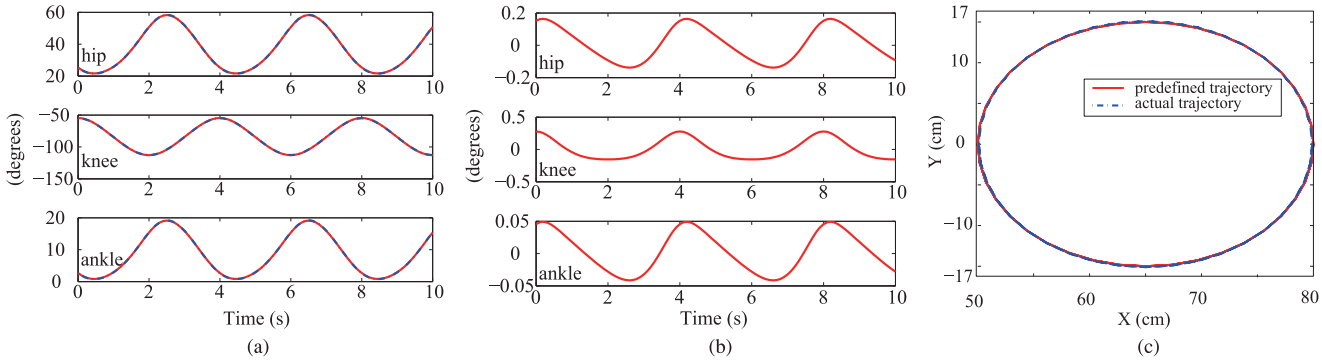

Fig. 7. Trajectory tracking performance of the passive training controller. (a) Actual (dashed lines) and predefined (solid lines) trajectories of each joint. (b) Tracking errors of each joint. (c) Tracking performance in the Cartesian plane.

TABLE IV
TRACKING ERRORS OF THE CYCLING MOVEMENT

Joint	$A_{\min}$ (°)	$A_{\max}$ (°)	$E_{\max}$ (°)	E_{rate} (%)
Hip	21.68	58.29	0.16	0.45
Knee	−112.89	−54.66	0.26	0.44
Ankle	0.84	19.14	0.05	0.27

TABLE V
DATA USED TO TRAIN AND TEST THE NEURAL NETWORK

Item	TF/GM			RF/BF			TA/GA		
θ_{hip} (°)	0	30	60	30	30	30	30	30	30
θ_{knee} (°)	−90	−90	−90	−30	−60	−90	−90	−90	−90
θ_{ankle} (°)	0	0	0	0	0	0	−10	0	20
Times	20	20	20	20	20	20	20	20	20

TABLE VI
SPECIFIC PARAMETERS OF THE NEURAL NETWORK

w_1	w_2	w_3	w_4	w_5	w_6	b_1	b_2	b_3
0.15	−0.11	0.31	−0.20	0.25	−0.30	0.06	−0.05	0.03

trajectory. The curves of tracking errors are shown in Fig. 7(b). Fig. 7(c) shows that the actual trajectory is an approximate ellipse which is very close to the desired circle in the Cartesian plane. The specific tracking errors are summarized in Table IV, where $A_{\min}$, $A_{\max}$, $E_{\max}$, and E_{rate} denote the minimum angle, maximum angle, maximum error, and error rate, respectively. The error rate E_{rate} is defined by

$$E_{\text{rate}} = \frac{E_{\max}}{A_{\max} - A_{\min}} \times 100\%. \tag{15}$$

Although the knee joint obtains the largest maximum error of $0.26°$, its tracking performance is still better than that of the hip joint due to a smaller error rate (see Table IV). Besides the parameters of the PI controller, the tracking error is also influenced by the joint moment of inertia. That is why, the ankle joint has the smallest error rate.

B. Active Training

The purpose of the active training evaluation is to test the agonist recognition rate of the proposed neural network, and to test the movement characteristics of the leg orthoses controlled by sEMG signals. sEMG signals from the tensor fasciae latae (TF), gluteus maximus (GM), rectus femoris (RF), biceps femoris (BF), tibialis anterior (TA), and gastrocnemius (GA) were acquired for this training evaluation.

1) Neural Network Training: Only the right leg was used for testing the agonist recognition. The subject sat in *iLeg* with the seat back adjusted to $150°$. Both legs were attached to the leg orthoses with strips of velcro, and the left leg kept a relaxed posture. The subject was asked to contract the selected muscles at three different postures (see Table V). Each muscle contraction lasted for 1–2 s and was repeated 60 times. The subject rested for 30 s every ten repetitions. Due to the leg orthosis keeping its posture during each repetition, the subject could only contract the leg muscles without moving the leg.

All sEMG signals were preprocessed before use (filtering, full-wave rectification, and smoothing, as in [27]). After preprocessing, sEMG signals were normalized by dividing the maximum amplitudes, which were acquired under the muscles' maximum voluntary contractile force. As there were 60 samples for flexion or extension of each joint, 120 samples were used for each perceptron. They were divided in half randomly. One part was used for neural network training, and the other was used for neural network validation. The delta rule was used to update the weights of the proposed neural network [23]. The parameters of the neural network after training are given in Table VI.

The trained neural network was validated by using the samples for validation, and the agonist recognition errors are shown in Table VII. The average recognition errors E_{mean} were $5.71\% \pm 1.30\%$, $4.05\% \pm 1.07\%$, and $3.06\% \pm 1.05\%$, respectively, for the hip, knee, and ankle. The errors were mainly caused by cocontraction of the antagonists, which happened when the maximum sEMG amplitudes were less than 30% of MVC.

2) Spring-Type Position Controller: Only the experiment on the knee joint is presented. According to (10), the reference joint angle θ_0 should be set firstly. To ensure the range of motion of

TABLE VII
AGONIST RECOGNITION ERROR

Joint	Posture 1 (%)	Posture 2 (%)	Posture 3 (%)	E_{mean} (%)
Hip	7.15	5.36	4.62	5.71 ± 1.30
Knee	5.26	3.65	3.23	4.05 ± 1.07
Ankle	3.52	3.80	1.85	3.06 ± 1.05

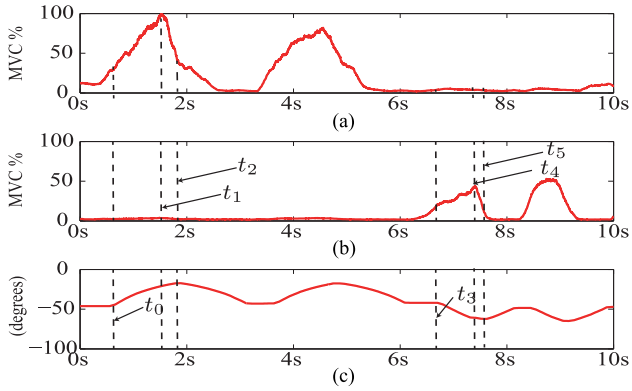

Fig. 8. Results of the spring-type position controller. (a) sEMG amplitudes of RF. (b) sEMG amplitudes of BF. (c) Knee joint angles of the leg orthosis.

the knee joint in both directions, it is better to set θ_0 near the middle of the knee joint. In this experiment, $\theta_0 = -46°$, which means that the knee joint will remain in this position unless the agonists are activated. Due to normalization of the sEMG amplitudes, each element of vector A in (10) is between 0 and 1; thus, the maximum angle from the reference joint angle is determined by the matrix K. When tuning K, we need to make sure that θ_d in (11) is in the range of motion of the leg orthosis. In this experiment, $K = 0.04$, which means that the maximum angle deviation from the reference joint angle is $K^{-1} = 25°$.

The results are shown in Fig. 8. At t_0, the RF was recognized as the agonist. The knee began to extend, and the extension movement led to the increase of the joint angle. At t_1, the sEMG amplitude of RF reached the maximum value. The extension movement did not stop until t_2 because the desired joint angle was always larger than the current joint angle between t_1 and t_2. After t_2, the knee began to move toward the reference angle due to the decrease of the sEMG amplitude of RF. Similarly, at t_3, the BF was recognized as the agonist, and the knee began to flex. Although the sEMG amplitude of BF began to decrease after t_4, the flexion movement did not stop until t_5. After t_5, the knee joint moved toward the reference angle when the sEMG amplitude of BF continued to decrease.

Fig. 8 shows that there is a delay of about 0.3 s between the control signals and the desired joint angle of the leg orthosis. The delay is mainly caused by the control loop rate f_c and the response time of the leg orthosis. The control loop rate is also the rate that the controller processes the sEMG signals. Due to the instability of sEMG signals, the leg orthosis tends to oscillate if the loop rate is too high. When tuning the loop rate, we should consider the tradeoff between the delay and oscillation. In this experiment, we get a feasible fixed loop rate of 6.67 Hz after repeated tests. The response time is also the time that the leg orthosis would take to finish the movement. Thus, it is relevant

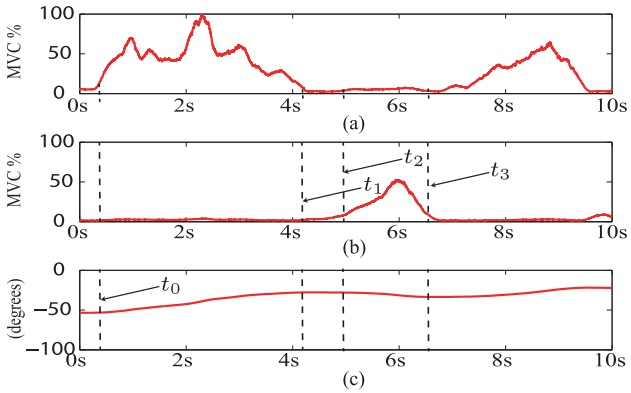

Fig. 9. Results of the damping-type velocity controller. (a) sEMG amplitudes of RF. (b) sEMG amplitudes of BF. (c) Knee joint angles of the leg orthosis.

to the matrix K and sEMG changes. The response time is always less than $1/f_c$. If the current movement is not finished in $1/f_c$, the controller will stop it and start the next loop.

3) Damping-Type Velocity Controller: Only data from the knee joint are presented. According to (8) and (9), the sEMG amplitudes are used to control the angular velocity of the leg orthosis, and the maximum angular velocity is determined by the matrix D. When tuning D, we need to make sure that D^{-1} does not exceed the maximum angular speed of the leg orthosis. Traditionally, we set the values of D according to the subject's subjective feelings. $D = 0.0625$; thus, we obtain the maximum angular velocity as $D^{-1} = 16$ °/s.

The results are shown in Fig. 9. Different from the spring-type position controller, this controller moved the leg orthosis continuously in the same direction until the agonists were exchanged or until the agonists were relaxed. The control loop rate of this controller was also 6.67 Hz. As shown in Fig. 9, the RF was recognized as the agonist at t_0, and the knee was controlled to move toward the direction of extension. The joint angular velocity changed with the sEMG amplitudes of RF during the movement, and the movement did not stop until the RF was relaxed (at t_1). Similarly, the BF was recognized as the agonist at t_2, and the knee was controlled to move toward the direction of flexion. This movement stopped at t_3 when the BF was relaxed.

V. DISCUSSION

In this paper, we have introduced a novel sitting/lying-type LLRR, namely *iLeg*. *iLeg* has a similar appearance to MotionMaker, but the mechanical structures and drive mechanisms of the leg orthosis are quite different. *iLeg* uses drive belts for energy transmission, whereas MotionMaker uses lead screw for energy transmission. By using the drive belts, the moment arm of each joint will remain unchanged during the joint movement. Besides, *iLeg* can adjust lengths of the thigh and crus by the associated electric length adjusting mechanism, which makes the leg orthosis more flexible. The purpose of developing *iLeg* is to replace rehabilitation bikes, which are widely used in China for training and rehabilitation of articular mobility and movement coordination, and provide more rehabilitation training methods for handicapped and hemiplegic patients. There are two main

differences between *iLeg* and the current popular LLRRs. One is the novel mechanism design, and the other is the passive and active training control methods. Thus, *iLeg* has not only all the functions of a rehabilitation bike, but also can provide sEMG-based active rehabilitation training methods. Because China has the largest population in the world, *iLeg* is expected to be widely used in China.

Compared with the standing/walking-type LLRRs, such as the Lokomat or LOPES, the training trajectories of *iLeg* are more diverse, such as cycling movement. This novel system may help patients perform uniarticular training, which provides convenience for targeted joint rehabilitation, such as foot drop. The sEMG-based impedance controllers detect not only the subject's movement intention, but also voluntary participation, which may encourage a patient to move his/her legs. Compared to existing techniques, the active training controllers proposed in this paper do not need the user to remember the relationship between the muscle contraction and the motion. Moreover, since the position or velocity of the leg orthosis is determined by the sEMG amplitudes, the user may try his/her best to contract the muscles to generate strong sEMG amplitudes during each rehabilitation session. Such voluntary participation could make the rehabilitation training more effective.

Muscle spasm should be considered seriously during active rehabilitation. The sEMG should be treated as abnormal signal when muscle spasm happens, and the controllers should stop *iLeg* immediately to avoid secondary damage to the subject. Although studies have suggested that substantial motor control information can be extracted from paretic muscles of stroke survivors by EMG signals [19], there are still many challenges when impaired subjects try and use *iLeg*. People with stroke and SCI typically are weak and have relatively small EMG amplitudes and abnormal muscle coordination patterns that may make it difficult for them to control *iLeg*. To deal with these challenges, we should focus on two aspects. One is choosing the appropriate EMG signals that can describe the motion intention of patients, and the other is improving the motion intention recognition algorithm. In our future work, we will focus on the clinical validation of this system.

ACKNOWLEDGMENT

The authors are grateful to Dr. Y. Hong, J. Zhang, and Z. Lu with the China Rehabilitation Research Center, Beijing, China, for providing suggestions.

REFERENCES

[1] G. Yan, H. Shen, X. Zhao, Q. Wei, Y. Kang, Z. Jia, L. Song, and M. Huang, "Effects of treadmill training on ADL of convalescent stroke patients," *Chin. J. Rehabil.*, vol. 22, no. 3, pp. 163–164, 2007.

[2] C. Schmitt, P. Métrailler, A. Al-Khodairy, R. Brodard, J. Fournier, M. Bouri, and R. Clavel, "The Motion Maker™: A rehabilitation system combining an orthosis with closed-loop electrical muscle stimulation," in *Proc. 8th Vienna Int. Workshop Funct. Elect. Stimul.*, Vienna, Austria, 2004, pp. 117–120.

[3] M. A. Maestro, A. E. Ruz, R. M. Casado-Lopez, A. M. Gonzalez, G. P. Mateos, E. G. Valdizan, and J. L. Martin, "Lokomat robotic-assisted versus overground training within 3 to 6 months of incomplete spinal cord lesion: Randomized controlled trial," *Neuralrehabil. Neural Repair*, vol. 26, no. 9, pp. 1058–1063, 2012.

[4] J. F. Veneman, R. Kruidhof, E. E. G. Hekman, R. Ekkelenkamp, E. H. F. van Asseldonk, and H. van der Kooij, "Design and evaluation of the LOPES exoskeleton robot for interactive gait rehabilitation," *IEEE Trans. Neural Syst. Rehabil. Eng.*, vol. 15, no. 3, pp. 379–386, Sep. 2007.

[5] S. Freivogel, J. Mehrholz, T. Husak-Sotomayor, and D. Schmalohr, "Gait training with the newly developed 'LokoHelp'-system is feasible for non-ambulatory patients after stroke, spinal cord and brain injury: A feasibility study, *Brain Injury*, vol. 22, nos. 7/8, pp. 625–632, 2008.

[6] G. R. West, "Powered gait orthosis and method of utilizing same," Patent 6 689 075, 2004.

[7] S. Hesse, C. Werner, D. Uhlenbrock, S. Frankenberg, A. Bardeleben, and B. Brandl-Hesse, "An electromechanical gait trainer for restoration of gait in hemiparetic stroke patients: Preliminary results," *Neurorehabil. Neural Repair*, vol. 15, no. 1, pp. 39–50, 2001.

[8] H. Schmidt, "HapticWalker—A novel haptic device for walking simulation," in *Proc. EuroHaptics*, Munich Germany, 2004, pp. 66–70.

[9] Y. Stauffer, Y. Allemand, M. Bouri, J. Fournier, R. Clavel, P. Metrailler, R. Brodard, and F. Reynard, "The WalkTrainer—A new generation of walking reeducation device combining orthoses and muscle stimulation," *IEEE Trans. Neural Syst. Rehabil. Eng.*, vol. 17, no. 1, pp. 38–45, Feb. 2009.

[10] E. Strickland, "Good-bye, wheelchair," *IEEE Spectr.*, vol. 49, no. 1, pp. 30–32, Jan. 2012.

[11] Rex Bionics REX web site, 2014. [Online]. Available: http://www.rexbionics.com

[12] A. Tsukahara, R. Kawanishi, Y. Hasegawa, and Y. Sankai, "Sit-to-stand and stand-to-sit transfer support for complete paraplegic patients with robot suit HAL," *Adv. Robot.*, vol. 24, no. 11, pp. 1615–1638, 2010.

[13] Argo Medical Technologies ReWalk web site, 2014. [Online]. Available: http://www.argomedtec.com

[14] B. H. Dobkin and P. W. Duncan, "Should body weight-supported treadmill training and robotic-assistive steppers for locomotor training trot back to the starting gate?" *Neurorehabil. Neural Repair*, vol. 26, no. 4, pp. 308–317, 2012.

[15] S. Freivoqel, D. Schmalohr, and J. Mehrholz, "Improved walking ability and reduced therapeutic stress with an electromechanical gait device," *J. Rehabil. Med.*, vol. 41, no. 9, pp. 734–739, 2009.

[16] P. Metrailler *et al.*, "Improvement of rehabilitation possibilities with the MotionMaker™," in *Proc. 1st IEEE/RAS-EMBS Int. Conf. Biomed. Robot. Biomechatron.*, 2006, pp. 359–364.

[17] M. Lotze, C. Braun, N. Birbaumer, S. Anders, and L. G. Cohen, "Motor learning elicited by voluntary drive," *Brain*, vol. 126, pp. 866–872, 2003.

[18] D. Leonardis *et al.*, "An EMG-controlled robotic hand exoskeleton for bilateral rehabilitation," *IEEE Trans. Haptics*, vol. 8, no. 2, pp. 140–151, Apr.–Jun. 2015.

[19] X. Zhang and P. Zhou, "High-density myoelectric pattern recognition toward improved stroke rehabilitation," *IEEE Trans. Biomed. Eng.*, vol. 59, no. 6, pp. 1649–1657, Jun. 2012.

[20] A. Roaas and G. B. J. Andersson, "Normal range of motion of the hip, knee and ankle joints in male subjects, 30–40 years of age," *Acta Orthopaedica Scandinavica*, vol. 53, pp. 205–208, 1982

[21] Y-C. Lin, M-J. J. Wang, and E. M. Wang, "The comparisons of anthropometric characteristics among four peoples in East Asia," *Appl. Ergonom.*, vol. 35, no. 2, pp. 173–178, 2004.

[22] N. Hogan, "Impedance control: An approach to manipulation: Parts I-III," *J. Dyn. Syst. Meas. Control*, vol. 107, no. 1, pp. 1–24, 1985.

[23] B. Widrow and M. E. Hoff, "Adaptive switching circuits," in *Proc. IRE WESCON Convention Rec.*, 1960, pp. 96–104.

[24] C. C. Cheah and D. Wang, "Learning impedance control for robotic manipulators," *IEEE Trans. Robot. Autom.*, vol. 14, no. 3, pp. 452–465, Jun. 1998.

[25] K. L. Michal, "The influence of early cycling training on balance in stroke patients at the subacute stage: Results of a preliminary trial," *Clin. Rehabil.*, vol. 20, no. 5, pp. 398–405, 2006.

[26] W. J. Thomas, J. M. Beltman, P. Elich, P. A. Koppe, H. Konijnenbelt, A. de Haan, and K. H. Gerrits, "Effects of electric stimulation-assisted cycling training in people with chronic stroke," *Arch. Phys. Med. Rehabil.*, vol. 89, no. 3, pp. 463–469, 2008.

[27] F. Zhang, P. Li, Z.-G. Hou, Z. Lu, Y. Chen, Q. Li, and M. Tan, "sEMG-based continuous estimation of joint angles of human legs by using BP neural network," *Neurocomputing*, vol. 78, no. 1, pp. 139–148, 2012.